

A Super-High-Frequency Non-Released Silicon Fin Bulk Acoustic Resonator

Mehrdad Ramezani^{#1}, Mayur Ghatge^{#2}, Valeriy Felmetzger^{*3}, Roozbeh Tabrizian^{#4}

[#]Electrical and Computer Engineering Department, University of Florida, USA

^{*}OEM Group, LLC., USA

¹mehram@ufl.edu, ²ruyam@ufl.edu, ³valeriy.felmetzger@oemgroupinc.com, ⁴rtabrizian@ufl.edu

Abstract— This paper reports, for the first time, on a high quality-factor (Q) super-high-frequency bulk acoustic wave resonator realized from integration of aluminum nitride (AlN) on sidewalls of a non-released single crystal silicon (Si) micro-fin. The non-released Fin Bulk Acoustic Resonator (FinBAR) enables monolithic integration of filters for realization of single-chip RF front-end (RFFE) modules. Benefiting from the low acoustic-loss of Si fin and large longitudinal piezoelectric coefficient of AlN, the FinBAR technology provides the high $k_r^2 \times Q$ required for implementation of wideband filters. Furthermore, having a frequency defined by the Si fin width, the FinBAR technology provides extreme lithographical scalability over the wide 3-30 GHz spectrum; hence facilitating chip-scale integration of multi-band spectral processors for carrier-aggregated RFFE. Proof of concept non-released FinBARs are fabricated through process optimization of magnetron sputtering to yield (0002)-textured AlN films on the sidewalls with perpendicular c-axis. The fin geometry is engineered to enable highly efficient acoustic energy localization in the active region to enhance resonator's $k_r^2 \times Q$. A non-released FinBAR at 4.2 GHz, with a Q of 1,573 and k_r^2 of 2.75% is demonstrated. The effects of c-axis misorientation of the sidewall transducer film and the non-released architecture of Si micro-fin on the resonator performance are discussed in detail.

Keywords—Fin bulk acoustic resonator, acoustic filters, carrier aggregation, 5G mobile communication.

I. INTRODUCTION

The mobile economy is experiencing a galloping growth in the number of users and also a flood of emerging technologies such as augmented and virtual reality, autonomous cars, smart homes and cities, and IoT, just to name a few. The ever-growing increase in the number of people using mobile networks and also an explosion in consumer propensity to adopt new technologies will rocket up the global data traffic to 110 Exabyte per month in 2023. Such upheaval in communication systems demands for a revolution in the infrastructure of wireless systems to provide enough bandwidth to transfer data at ultra-high speeds [1]. To accommodate more capacity for enormous data traffic demands, communication systems are planning to go beyond the 4G spectrum (i.e. sub-6 GHz) and take full advantage of the current resources by using new methods of channel allocation and carrier aggregation.

Realizing such transformations in current communication systems requires radically new integrated resonator technology that enables (1) extreme frequency scalability to cm- and mm-wave regime while sustaining high performance, (2) on-chip / lithographical frequency scalability to accommodate multi-frequency / -band carrier aggregation for 5G data

communication protocols, and (3) monolithic integration with CMOS to substantially avoid excessive noise and interference at shorter wavelength (i.e. cm- and mm-wave) regimes. Such a technology does not exist today and available RFFE rely on piezoelectric film bulk acoustic wave (BAW) resonators that entirely lack the required specifications. Piezo-film BAW resonators are planar devices that require releasing / air-cavity or integration on multi-layered Bragg reflectors to yield high Q . Neither of these platforms are readily available in CMOS manufacturing. Furthermore, suffering from planar architecture, piezo-film BAW resonators require large foot-prints to yield required transduction area for low-loss operation. Moreover, the resonance frequency of these devices is tightly tied to their thickness and cannot be tailored lithographically; hence, preventing integration of multi-frequency and multi-band resonators needed for carrier aggregated systems. Finally, extreme frequency scaling of piezo-film BAW resonators requires radical miniaturization of the film thickness, which (1) is not readily possible in current piezo-film deposition technologies and (2) results in significant degradation of the resonator Q [2].

To surpass the fundamental challenges with current piezo-film BAW resonators, this paper presents the radically new non-released Fin Bulk Acoustic Resonator (FinBAR) technology that targets transformation of RFFE for 5G systems. The new technology is based on integration of highly (0002)-textured AlN film on the sidewalls of an acoustically engineered fin directly carved on the silicon substrate (Fig. 1). The non-released FinBAR can be monolithically integrated post-CMOS and benefits from lithographical frequency scalability through changing the Si fin width. Benefiting from

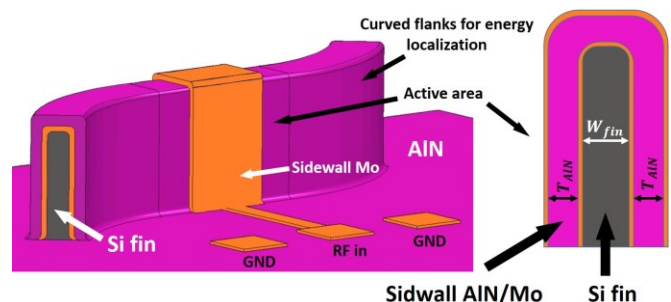


Fig. 1. Conceptual schematic of the non-released Si FinBAR. An acoustically engineered fin is patterned in single crystal Si substrate and covered by piezoelectric AlN film and metal electrodes. The non-released FinBAR provides: (1) high- $k_r^2 \times Q$ over the entire SHF regime, (2) lithographical frequency scalability, (3) post-CMOS monolithic integration; hence, enables transformation of integrated RFFE for 5G wireless systems.

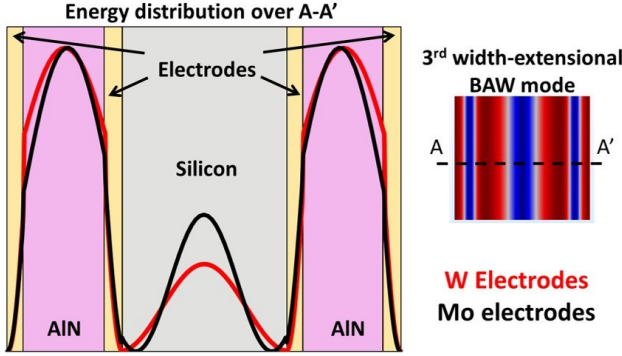


Fig. 2. The cross-sectional acoustic energy distribution across the FinBAR active region for different electrode materials. Mo is used since it yields the highest energy concentration in AIN and enhance the k_t^2 .

low acoustic-loss in single crystal Si and large longitudinal electromechanical coupling (i.e. e_{33}) of sidewall AIN, non-released FinBAR provides a large $k_t^2 \times Q$ sustainably over the entire super-high-frequency regime (i.e. 3-30 GHz). Furthermore, benefiting from large sidewall area for transduction, low-loss FinBARs with different frequencies can be implemented in small planar footprint and integrated in arrays to realize chip-scale multi-frequency / multi-band RFFE.

II. FINBAR CONCEPT

FinBAR is formed from a high-aspect-ratio fin that is patterned on a single crystal Si substrate and subsequently covered by piezoelectric transduction layer that has one or two metallic layers on either side to serve for application of RF signal. FinBAR is operating in width-extensional bulk acoustic mode, where the resonance frequency is defined by the Si fin width and sidewall transduction stack thickness.

Having a multilayered structure, the resonance frequency of the $2n+1$ harmonic is defined by:

$$f_{2n+1} \cong \frac{2n+1}{2} \left(\frac{2T_{AIN}}{V_{AIN}} + \frac{W_{fin}}{V_{Si}} + \frac{2T_{electrodes}}{V_{electrodes}} \right)^{-1} \quad (1)$$

Here $T_{AIN,electrodes}$ and W_{Fin} are the thickness of AIN piezoelectric film and metal electrodes on the sidewalls and width of the Si fin, respectively; and $V_{AIN,electrodes}$ and V_{Si} are longitudinal acoustic wave velocities in AIN, metal electrodes and Si, respectively. Therefore, FinBARs having resonance frequencies spread over a wide spectrum can be achieved by forming fins with different widths. In contrast to piezo-film BAW resonators, which have acoustic energy majorly concentrated in the piezoelectric film, in FinBARs, a considerable portion of the acoustic energy is contained in Si fin. Such energy distribution is the key factor in delimiting the Q and k_t^2 of the resonators; hence, the optimum ratio of piezoelectric and metal thicknesses to the Si fin width and also the appropriate harmonic number (i.e. $2n+1$) should be found to optimize resonator performance at a desired frequency. While the k_t^2 is defined by the relative energy distribution in piezo-layer versus other mechanically passive layers, to achieve the maximum k_t^2 , the optimum ratio of layers' thicknesses and also the harmonic number should be found. As a starting point in

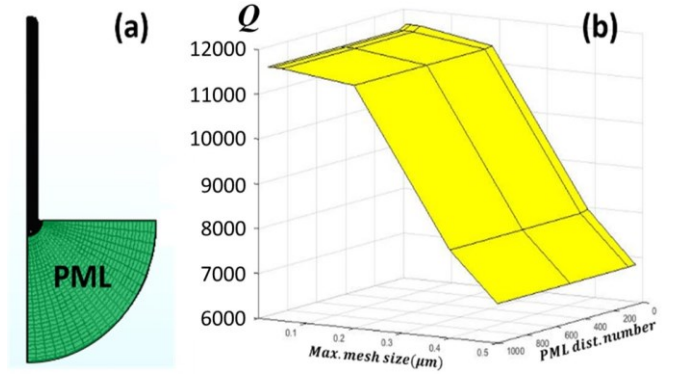


Fig. 3. (a) The meshing distribution in the quarter of the FinBAR used in FEM models to extract the anchoring Q . PML region is shown in green and it has coarser mesh compared to the device section. (b) Simulated Q vs increasing the mesh density, both in the PML and also the FinBAR. The extracted Q converges to a specific value beyond a certain densification level.

design, for the WE_{2n+1} width-extensional mode, the optimum Si fin width can be estimated from:

$$W_{fin,opt} = (2n - 1) \frac{V_{Si}}{V_{AIN}} T_{AIN} \quad (2)$$

In (2), the effect of electrodes on k_t^2 is ignored. In practice, aside from the relative thickness / width of Si fin and AIN layer, electrode material selection is also a key factor in defining the performance of FinBARs. Opting for proper electrode material, the relative energy distribution in AIN can be enhanced, which results in an improved k_t^2 . Finally, opting for proper crystallographic orientation of the Si fin, the k_t^2 of FinBARs can be further optimized. Fig. 2 demonstrates the energy distribution over the FinBAR cross-section for different electrode materials (Molybdenum (Mo) and Tungsten (W)). While the higher energy distribution in AIN results in higher k_t^2 , it should be noted that such an increase results in lower energy density in Si fin, which degrades the resonator Q . Therefore, there exist a trade-off between k_t^2 and Q in a FinBAR: more energy in the semiconductor fin that has low acoustic dissipation results in higher Q , while it reduces the amount of energy in transducer and results in lower k_t^2 . In this paper, a ~ 4.2 GHz FinBAR operating in 3rd width-extensional BAW mode is implemented, through integration of 1 μ m-thick sidewall AIN film on $\langle 100 \rangle$ -aligned Si fin with a width of 1 μ m.

III. NON-RELEASED FINBAR

Conventional micromechanical resonators, including piezo-film BAW, are mostly released and are clamped through narrow tethers to minimize the acoustic energy leakage and enhance the Q . Recently, released FinBARs have been demonstrated, which do not lend themselves to CMOS monolithic integration [3]. In this paper, the non-released architecture is demonstrated, for the

Table 1. Simulated anchoring Q and theoretical acoustic / intrinsic Si and AIN Q for 4.2 GHz FinBARs aligned to different crystallographic orientations.

Orientation	Anchor Q	Si Q	AIN Q	Overall Q
$\langle 100 \rangle$	6,200	33,000	3,000	4,187
$\langle 110 \rangle$	90,000	11,000		5583
$\langle 111 \rangle$	20,000	4,900		3565

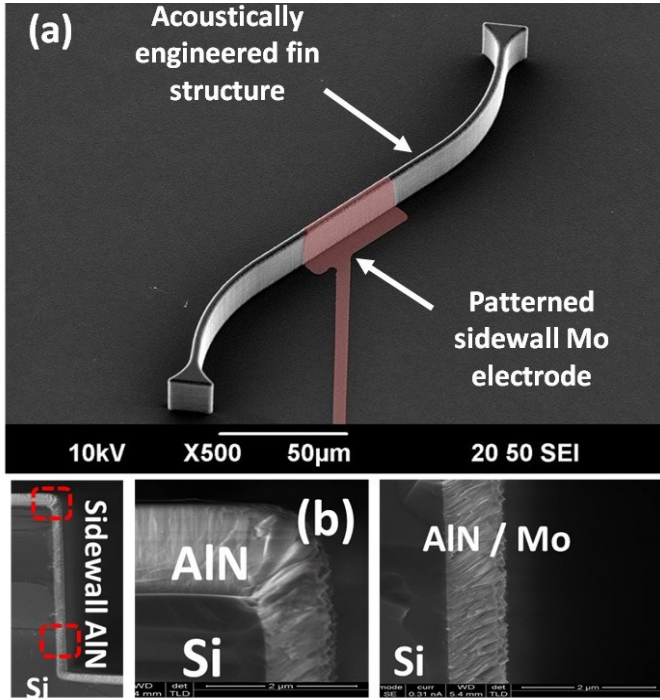


Fig. 4. (a) The SEM of the fabricated non-released FinBAR. (b) The cross-sectional SEM of the FinBAR in active region. The thickness of AIN / Mo on sidewall is nearly half of the layers on the top surface. The continuity of the films across the Si fin corners is evident.

first time. Perfectly Matched Layers (PML) are used to identify the effect of anchoring in non-released FinBARs on the overall Q . Fig. 3 demonstrates the simulated Q over PML distribution number and mesh size. Various combinations of PML distribution and mesh size are used to identify a reliable result for anchoring Q . Table I compares the simulated anchoring Q for FinBARs aligned to different crystallographic orientation of single crystal Si. Besides the anchoring, the Q corresponding to acoustic dissipation at operation frequency (i.e. 4.2 GHz) in Si fin is also extracted from [2]. As evident in Table 1, while FinBARs aligned to $\langle 100 \rangle$ crystallographic direction has the highest acoustic / intrinsic Q , the optimum Q corresponds to the FinBAR aligned to $\langle 110 \rangle$ orientation. While the simulated anchor loss demonstrates the high Q despite of non-released architecture of the FinBAR, the acoustic energy leakage can be further reduced through increasing the fin width at anchoring face to create an additional acoustic impedance mismatch.

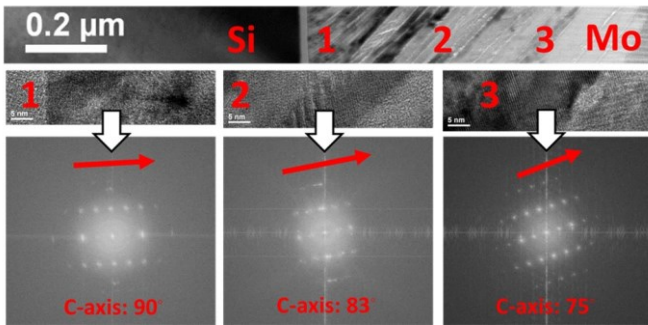


Fig. 5. The TEM of sidewall AIN at different regions across the thickness. The c-axis tilts from perpendicular at the Si interface to 75° at the top Mo interface.

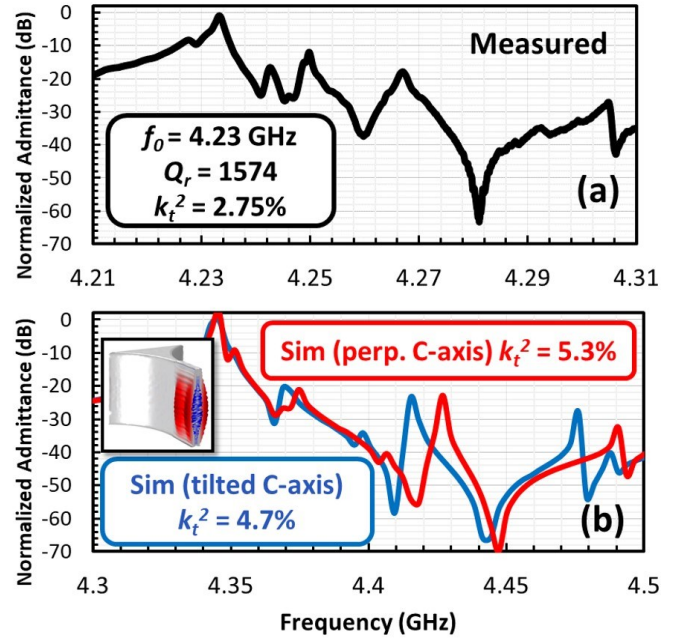


Fig. 6. The (a) measured and (b) simulated admittance of the non-released FinBAR using COMSOL. Simulations are done for both perfectly perpendicular and practically tilted c-axis scenarios.

IV. DEVICE FABRICATION AND CHARACTERIZATION

FinBARs are fabricated through a simple process started with forming the high-aspect-ratio fins by etching the semiconductor substrate using Bosch DRIE process. This process results in fins with rough sidewall surfaces with large scallops, which is not suitable for deposition of (0002)-textured AIN film with desired crystallographic orientation. Hence, a high temperature hydrogen (H_2) annealing is performed to achieve mirror-smooth sidewall surface. Next step is single deposition of magnetron sputtered AIN film followed by Mo layer to serve as the top electrode. Proper tuning of the process is used to enable highly (0002)-textured AIN piezoelectric film on the sidewall with perpendicular c-axis and uniform thickness across the fin height. The process is followed by patterning top Mo on the sidewall and AIN layer on the Si through RIE, to realize RF (Mo) and ground (heavily p-doped Si) pads for the application of RF electrical signal. Figure 4 (a), demonstrates the SEM of the fabricated device and RF pads. Perfectly patterned sidewall Mo electrode is evident. Fig. 4 (b) shows the cross-sectional SEM of the FinBAR in active region, highlighting the rounded corner of Si fin after H_2 annealing and continuity of AIN and Mo films from top surface to sidewall. Fig. 5 shows the high-resolution TEM images of sidewall AIN in different regions across film thickness. The c-axis crystallinity is evident from FFT of these images. Also, it is worth noting that the c-axis is tilting continuously across the film thickness. While a nearly perfect perpendicular c-axis is achieved at the interface with Si fin, the c-axis is tilted to $\sim 75^\circ$ at the top surface of AIN (i.e. interface with top Mo). Such a tilt slightly degrades the resonator k_t^2 and may induce shear-based spurious modes. Fig. 6 (a) demonstrates the measured admittance of the non-released FinBAR operating at 4.23 GHz. The admittance is extracted after de-embedding the resistance

of bottom electrode (i.e. p-doped Si) and shunt capacitance under Mo pad used for GSG probing. A Q of 1,574 and kt^2 of ~2.75% is measured for the FinBAR. The lower Q compared to simulations and analytical predictions can be attributed to rough surface of AlN / top Mo on the sidewall, and additional energy dissipation mechanisms corresponding to piezoelectric film [4]. Fig. 6 (b) compares the COMSOL simulated admittance of FinBARs with perpendicular and tilted c-axis configuration that follows / mimics the TEM characterization results. The c-axis tilt from 90° to 75° over the sidewall film thickness results in degradation of the kt^2 from 5.3% to 4.7%. Also, the lower kt^2 of the measured / implemented FinBAR (i.e. 2.75%) compared to COMSOL model (i.e. 4.7%) can be attributed to the non-ideal crystallinity of the sidewall AlN film as well as imperfect acoustic energy localization in the active / electrode region of the device.

V. CONCLUSION

This paper presents the super-high-frequency (SHF) non-released Fin Bulk Acoustic Resonator (FinBAR) technology for the first time. This technology is formed from integration of highly (0002)-textured AlN piezoelectric film on the sidewall of non-released single crystal Si fin. The non-released FinBAR technology provides transforming characteristics including: (1) monolithic integration with

CMOS; (2) high $kt^2 \times Q$ over the entire SHF regime; and (3) lithographical frequency scalability. These unique features pave the way for implementation of fully integrated multi-frequency and multi-band RF front-end modules for carrier aggregated 5G wireless systems. Detailed design, simulation and fabrication process for a 4.23 GHz non-released FinBAR is presented. The proof of concept device demonstrates a kt^2 of 2.75% and a Q of 1,574.

ACKNOWLEDGEMENT

This work was supported in part by NSF grants ECCS 1752206. The authors would like to thank Nanoscale Research Facility staff at the University of Florida and Nicholas Rudawski for help with TEM.

REFERENCES

- [1] Ruby, Rich. "A snapshot in time: *The future in filters for cell phones*." IEEE Microwave Magazine 16.7 (2015): 46-59.
- [2] Tabrizian, et. al., 2009, June. In Solid-State Sensors, Actuators and Microsystems Conference, 2009. TRANSDUCERS 2009. International (pp. 2131-2134). IEEE.
- [3] Ramezani, M., M. Ghatge, and R. Tabrizian. "High- Q silicon fin bulk acoustic resonators." IEEE IEDM 2017.
- [4] Tabrizian, R., & Rais-Zadeh, M. (2015, June). *The effect of charge redistribution on limiting the $kt^2 \cdot Q$ product of piezoelectrically transduced resonators*. In 2015 Transducers-2015 18th International Conference on Solid-State Sensors, Actuators and Microsystems (TRANSDUCERS) (pp. 981-984).